Shear-Induced Unfolding of Lysozyme Monitored In Situ

Lorna Ashton,[†] Jonathan Dusting,[‡] Eboshogwe Imomoh,[‡] Stavroula Balabani,[‡] and Ewan W. Blanch[†*]
[†]Manchester Interdisciplinary Biocentre & Faculty of Life Sciences, University of Manchester, Manchester M1 7DN, United Kingdom; and [‡]Experimental and Computational Laboratory for the Analysis of Turbulence (ECLAT), King's College London, Strand, London WC2R 2LS, United Kingdom

ABSTRACT Conformational changes due to externally applied physiochemical parameters, including pH, temperature, solvent composition, and mechanical forces, have been extensively reported for numerous proteins. However, investigations on the effect of fluid shear flow on protein conformation remain inconclusive despite its importance not only in the research of protein dynamics but also for biotechnology applications where processes such as pumping, filtration, and mixing may expose protein solutions to changes in protein structure. By combining particle image velocimetry and Raman spectroscopy, we have successfully monitored reversible, shear-induced structural changes of lysozyme in well-characterized flows. Shearing of lysozyme in water altered the protein's backbone structure, whereas similar shear rates in glycerol solution affected the solvent exposure of side-chain residues located toward the exterior of the lysozyme α-domain. The results demonstrate the importance of measuring conformational changes in situ and of quantifying fluid stresses by the three-dimensional shear tensor to establish reversible unfolding or misfolding transitions occurring due to flow exposure.

INTRODUCTION

The unfolding of proteins induced by externally applied physiochemical parameters has been widely investigated, and although the exact mechanisms remain elusive, new insights into protein dynamics have been achieved. Numerous proteins, including the well-studied protein hen lysozyme, have been shown at acidic pH and with prolonged heating to form fibrils similar to those responsible for diseases such as Alzheimer's, Parkinson's, and type II diabetes (1–3). However, despite numerous investigations, it is unclear as to whether or not fluid shear flows can also be exploited to induce conformational changes or unfolding in proteins. Fluid shear-induced unfolding has been reported in certain proteins, including von Willebrand Factor (4,5), β-lactoglobulin (6,7), and glycoprotein Ib (8), yet alternative studies imply that proteins will not unfold under high shear rates (9). A crucial problem with shear-induced unfolding is a lack of conclusively characterized protein behavior as a function of relevant hydrodynamic parameters, including spatiotemporal velocity and stress distributions. A further limitation of many previous studies is that they have relied on techniques that are unable to measure the conformational characteristics of proteins during their exposure to shear, meaning that any reversible changes could not be detected.

To overcome both of these important limitations, we combined two powerful laser techniques, Raman spectroscopy and particle image velocimetry (PIV), to experimentally study shear dependency of lysozyme in a more controlled manner than had hitherto been undertaken. Lysozyme consists of 39% helical structure and 10% β-sheet (PDB database, 1LSE) in two domains, α and β. The α-domain is rich in α-helical structure with four α-helices, A, B, C, and D, and a 3_{10} helix, whereas the β-domain contains β-sheet, several loops, and a further 3_{10} helix. Thermal unfolding and aggregation of human and egg-white lysozyme have been extensively documented (1,3) and characterized by Raman spectroscopy (10,11). Raman spectroscopy is increasingly being applied to protein conformational studies in solution not only because of its sensitivity to changes in secondary structure and hydrophilic exposure of side chains, but also for its ability to determine the presence of more disordered structures such as PPII helix, which is now recognized as a common structural motif in unfolded states (12–15). By using Raman spectroscopy to monitor protein structure in flow, it should be possible to identify any flow-induced conformational changes that occur during and after flow has ceased, thereby monitoring reversible and nonreversible changes. PIV is an established image-based technique used to resolve time-dependent velocity fields and provide accurate estimates of stress magnitudes and distributions (16). In this study, PIV has been employed to characterize the flow conditions to which proteins were exposed, so that the behavior of proteins can ultimately be described as a function of these conditions.

METHODS

Taylor-Couette flow cell

A Taylor-Couette flow cell suitable for laser-based diagnostic techniques was developed to expose proteins to well-controlled fluid stresses. As shown schematically in Fig. 1, the flow cell consisted of two concentric cylinders, a stationary glass outer cylinder and a rotating Teflon inner cylinder. The radii of the inner and outer cylinders were 20.6 mm and 25.5 mm, respectively. The height of the cylinders, H, was 55 mm, with a characteristic aspect ratio of $H/d = 11.2$, where d is the annular gap distance (4.9 mm). Similar Taylor-Couette flow cells have been used in previous protein studies

Submitted December 10, 2008, and accepted for publication February 13, 2009.

Lorna Ashton and Jonathan Dusting contributed equally to this work.

*Correspondence: e.blanch@manchester.ac.uk

Editor: Kathleen B. Hall.

0006-3495/09/05/4231/6 $2.00

doi: 10.1016/j.bpj.2009.02.024

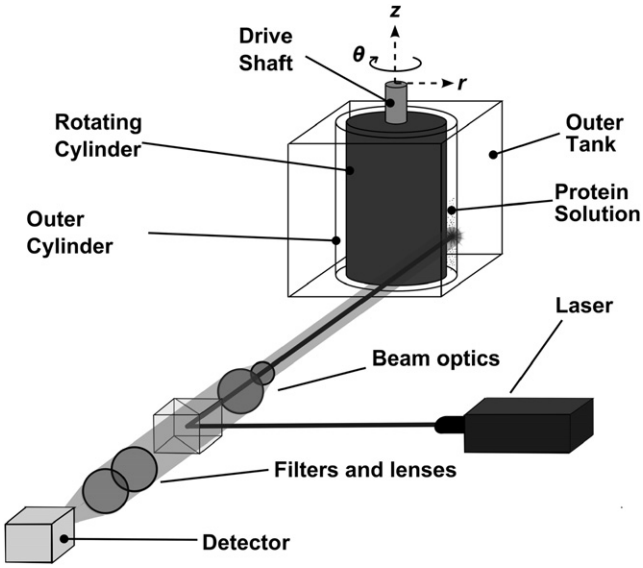

FIGURE 1 Schematic of experimental setup, including flow cell and Raman spectroscopy laser and optics.

(17) as well as in other biological applications (18–20). The circulating, pump-free, self-contained nature of the flow system is ideal for monitoring protein behavior with Raman spectroscopy because protein solutions can be exposed continuously to controlled shear environments.

Raman spectroscopy

Separate experiments were conducted with lysozyme dissolved in 100% water and then in 95% glycerol solution. Hen egg-white lysozyme was purchased from Sigma (St. Louis, MO) (L6876 containing 95% protein by weight with the remainder being sodium acetate and sodium chloride buffer salts) and used without further purification. The dry material was dissolved in distilled deionized H_2O at a concentration of 10 mg/mL, with a measured pH of 4.0 (HANNA Instruments pH209 meter (Woonsocket, RI)), which is below physiological pH but well above that required to unfold hen lysozyme at room temperature (21–23). Raman measurements were performed using a ChiralRAMAN spectrometer (Biotools, Jupiter, FL) with the following experimental conditions used for both the lysozyme in water and lysozyme in glycerol experiments: laser wavelength 532.5 nm, spectral resolution ~7 cm^{-1}, illumination period 0.6615 s. All spectra were acquired for 93 scans totaling 1.01 min. The laser power for the lysozyme in water was 0.60 W at the sample and 0.10 W for lysozyme in glycerol because of the large signals from the glycerol background. A reference spectrum was first collected under stationary conditions and then with the flow cell inner cylinder driven at rotational speeds of 30, 60, 90, 120, and 150 rpm. A stepper motor (Smart-Drive, Cambridge, UK) with a resolution of 52,000 microsteps/revolution was used to control the rotational speed of the inner cylinder. A final spectrum was collected as soon as the cylinder stopped rotating.

Data pretreatments

Data pretreatments of solvent subtraction, baseline subtraction, and smoothing, applied with Origin 7.5 software (OriginLab, Northampton, MA), were essential to compare the two different spectral sets monitoring lysozyme in 100% water and lysozyme in 95% glycerol. As can be observed in Fig. 2, *a* and *b*, both sets of raw data had large but different solvent backgrounds. By subtracting the appropriate solvent spectrum recorded for each of the flow speeds, the water background and bands arising from glycerol were greatly reduced, particularly in the region of 1540–1700 cm^{-1}, where the intensity of water and glycerol backgrounds was far lower than that observed for other regions of the spectra. Baseline subtraction was performed individually for each spectrum to remove baseline drift as a result of the different flow rates and instrument instabilities. Electronic smoothing using a fast Fourier transform at two fast Fourier transform points was also applied to reduce noise.

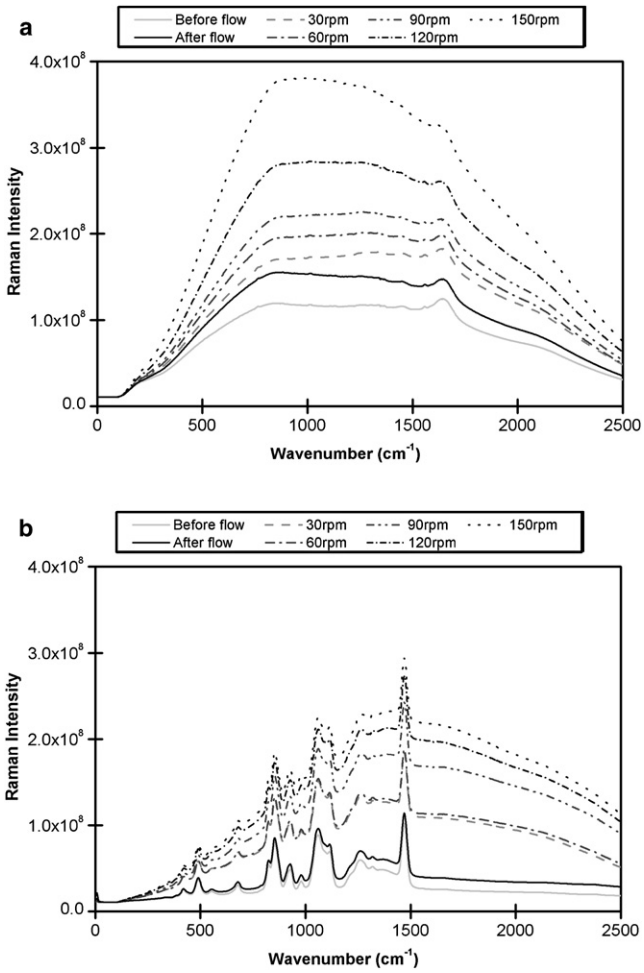

FIGURE 2 Raw Raman spectra of lysozyme in 100% water (*a*) and lysozyme in 95% glycerol and 5% water (*b*), recorded without flow, at increasing rates of flow and immediately after flow was stopped.

PIV

Velocity fields were obtained using a time-resolved PIV system (Dantec Dynamics, Bristol, UK). The measurement plane was illuminated with a pulsed Nd:YAG laser with a wavelength of 532 nm and a maximum output of 25 mJ. Image pairs of 1024 × 1280 pixel resolution were captured using an IDT (San Jose, CA) XS-3 CMOS camera and timing box. An adaptive cross-correlation was used with a final window size of 32 × 32 pixels and 50% window overlapping. The resulting velocity fields included measurements over the full vessel height at 11 locations radially distributed across the annulus. This measurement density was found to adequately resolve the flow topologies associated with the different flow rates and solvents used in this study.

RESULTS AND DISCUSSION

Fig. 3, *a* and *b*, display pretreated Raman spectra from ~1540 to 1700 cm^{-1} at different flow rates of lysozyme in water and

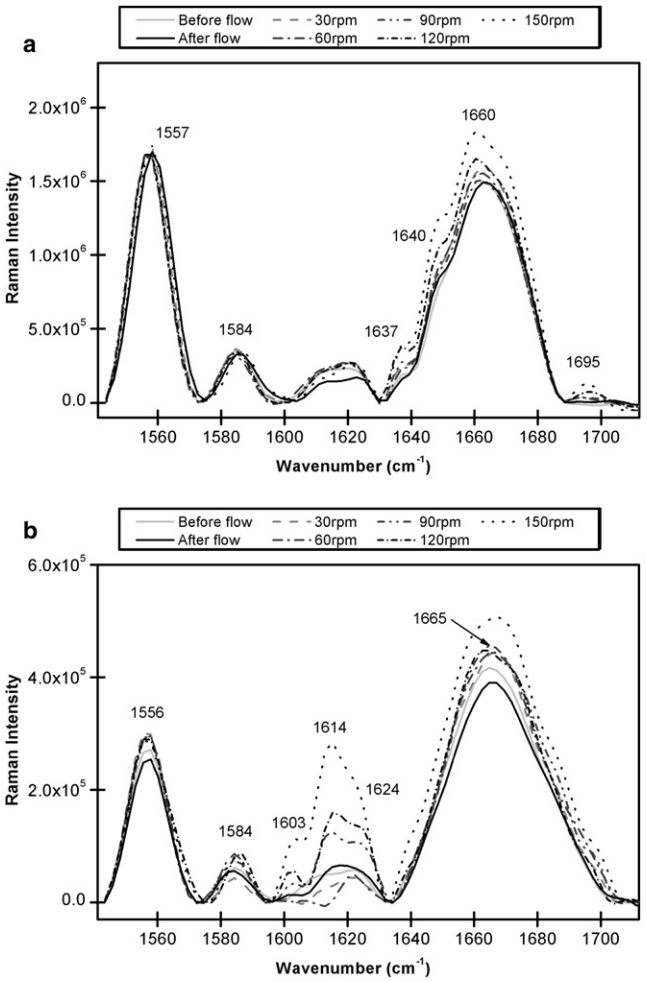

FIGURE 3 Raman spectra of lysozyme in 100% water (*a*) and lysozyme in 95% glycerol and 5% water (*b*), recorded without flow, at increasing rates of flow and immediately after flow was stopped.

lysozyme in 95% glycerol, respectively, and reveal changes in band profile and intensity. These spectral variations show that in fluid flow, conformational changes do occur in the lysozyme molecules, although to differing degrees, depending on solvent and rotation rate. In both experiments, an increase in intensity and band width in the amide I frequency (1640–1680 cm^{-1}) arising from the C = O stretching of the peptide CONH groups can be observed as Ω increases. The broadening of bands has previously been associated with denaturation of proteins (10,24), suggesting that some unfolding of the lysozyme native structure is occurring as shear rates are increased. In Fig. 3, *a* and *b*, the spectral profile after the flow is stopped is similar to the initial reference spectrum, indicating that the changes in lysozyme conformation occurring with flow are reversible. Thermal denaturing of lysozyme has also been reported as fully reversible at temperatures below 75°C when only brief periods of heating are used (10,11). Reversible conformational changes were also observed by Lee and McHugh (25) in the helix-to-disordered transition of poly-L-lysine in an 87.5% methanol-water solution in simple shear flow as monitored by flow birefringence and modulated polarimetry. They observed that helical structure refolded within 20 s of flow stopping and suggested this may be because of a combination of chain relaxation and reformation of hydrogen bonds.

Differences in variations can be observed between the two sets of spectra in Fig. 3. In Fig. 3 *a*, the largest intensity variations can be observed in the region ~1630–1700 cm^{-1}, the spectral region associated with elements of secondary structure, whereas in Fig. 3 *b*, the most significant changes can be observed in the region ~1575–1635 cm^{-1}, associated with side-chain interactions. The temperature and thermodynamic properties associated with thermal denaturation of lysozyme have previously been shown to be dependent on the composition of glycerol/water mixtures (26). This is most likely due to differences in molecular hydration properties near the protein surface that result as a function of solvent composition (27,28) and may affect the behavior of lysozyme in flow. However, differences in the fluid dynamic properties for the two cases may also be significant when considering the varying conformation changes observed in water and in glycerol. Although both solutions have similar shear rates (γ), they differ considerably in shear stress magnitude (τ). The dynamic viscosity (μ) of glycerol solution at 24°C is ~430 times greater than that of water, and because τ is simply the product of μ and γ, the shear stress magnitudes were much larger for the glycerol experiments. Furthermore, the Taylor-Couette flow cell generates significant differences in flow topology and stress distribution for the different solutions. As is well documented, several different flow regimes occur as a function of Reynolds number, $Re = r_i d\Omega\rho/\mu$, where r_i is the inner cylinder radius and ρ is the fluid density (29). The most significant flow regime transition occurs at the critical Re number, which is ~98 for the current flow cell (30). For $Re < 98$, the flow is in the Couette flow regime, which is time invariant, axisymmetric, and purely in the azimuthal (θ) direction, i.e., with no radial (r) or axial (z) component. For the glycerol flow experiments, Re varied between ~1.1 and 5.7, so even at $\Omega = 150$ rpm, there was Couette flow. With water as the solvent, Re varied from ~330 to 1618, well above the critical value. Because of the complex nature of supercritical flows, the time-resolved two-dimensional flow field in water was quantified using PIV. The meridional plane velocity field corresponding to $\Omega = 30$ rpm is shown in Fig. 4. A Taylor vortex flow (TVF) pattern is captured by the measurements, characterized by axisymmetric counter-rotating vortices (Taylor vortices) stacked in the axial direction, with radial inflows and outflows located between each vortex. Furthermore, PIV results obtained at higher rotation rates indicate that above $\Omega = 90$ rpm, the flow is variable with time, with an oscillatory motion characteristic of the wavy vortex flow (WVF) regime, which occurs at higher Re values (29).

For shear experiments with water (Fig. 3 *a*), bands increasing in intensity were observed at ~1637, 1640, 1660,

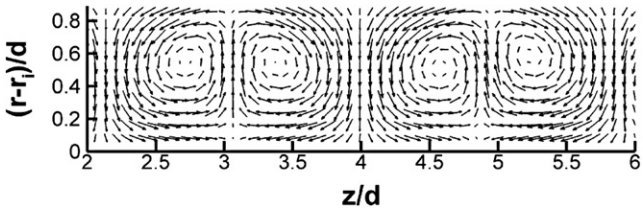

FIGURE 4 Meridional plane mean velocity vector field measured using PIV for water, $\Omega = 30$ rpm, in the axial region $2.0 \leq z/d \leq 6.0$, where $z/d = 0$ corresponds to the bottom of the flow cell. The vector field is oriented such that the inner cylinder is located at the bottom of the figure. The velocity field shown here is the ensemble average of 3000 instantaneous vector fields.

and 1695 cm^{-1}. Research by Takekiyo et al. (31) suggests that bands at ~1637 cm^{-1} and 1640 cm^{-1} are associated with solvated α-helical structure, whereas bands at ~1655 cm^{-1} arise from buried α-helical structure. Shear-induced conformational changes appear to occur in the α-helical structure of lysozyme in water but not in 95% glycerol (Fig. 3 *b*). The band at ~1695 cm^{-1} is assigned to β-structure (32), further indicating changes in backbone structure in water as flow rate increases. The increasingly complex TVF and WVF regimes may initiate a loss of backbone structure in the lysozyme molecules, which does not occur in the simpler Couette flow of the glycerol experiment. However, the differences between Fig. 3, *a* and *b*, are most noticeable for bands at ~1556, 1584, 1603, 1614, and 1624 cm^{-1}, which increase in intensity as Ω increases for lysozyme in 95% glycerol but not lysozyme in water. The largest intensity increases can be observed in Fig. 3 *b* in the phenylalanine-assigned band at ~1603 cm^{-1} (33,34) and the tyrosine-assigned bands at ~1614 cm^{-1} and 1624 cm^{-1} (24,33,34). Further changes, albeit to a lesser extent, can be observed in the bands measured at ~1556 cm^{-1} and 1584 cm^{-1}, which are assigned to tryptophan residues. As shown in Fig. 5, the three phenylalanine residues and the three tyrosine residues appear to be situated toward the exterior of the lysozyme structure, compared with the six tryptophan residues that are closer to the protein's core. The observed changes suggest that the considerable viscous shear stresses alter the conformation or geometry of the more exteriorly located residues to a greater extent than the more centrally located tryptophan residues (32,34). Furthermore, the change in solvent exposure of residues Phe-38, Phe-34, Tyr-23, and Tyr-20 suggests that the main structural changes occurring in glycerol are located in the α-domain, particularly in α-helix B. The relative lack of change in the environment of the tryptophan residues, in particular Trp-62 and Trp-63, further illustrates that in 95% glycerol, large conformational changes occur less in the β-domain than in the exterior regions of the molecule, which are probably affected more by the higher shear stresses.

As noted in the Introduction, the ability for fluid flow to drive protein unfolding has been questioned recently. One interesting study is that of Jaspe and Hagen (9), who used

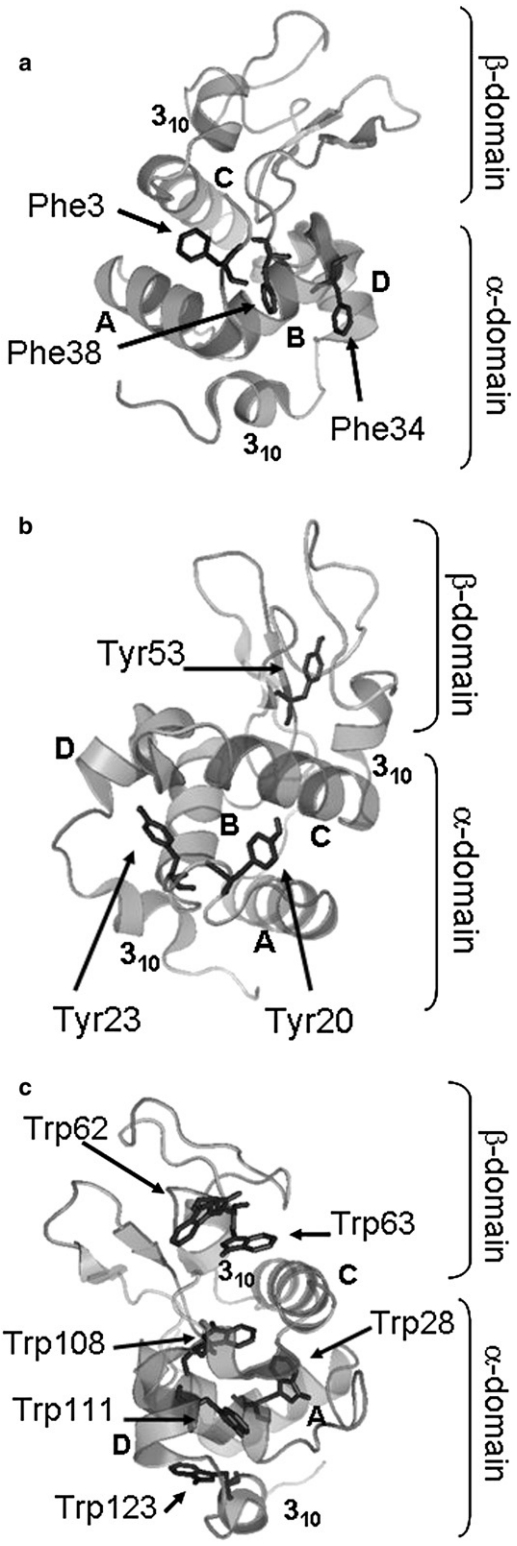

FIGURE 5 Cartoon representation of the structure of hen egg-white lysozyme drawn from atomic coordinates in the PDB (1LSE) using PyMOL. Phenylalanine (*a*), tyrosine (*b*), and tryptophan (*c*) residues are shown.

fluorescence to analyze solutions of cytochrome *c* being pumped through small-diameter cylindrical tubes but were unable to detect protein unfolding. They then used a basic model to propose a required minimum shear rate of $\gamma = 10^7\ s^{-1}$ to unfold typical globular proteins in ''simple'' shear flows, and speculated that previous examples of shear-induced unfolding could be attributed to unusual circumstances. However, the results observed in this study with glycerol as the solvent demonstrate that relatively stable, globular proteins may, in fact, undergo conformational changes when exposed to a simple, laminar, flow regime. Furthermore, the shear rates are relatively low: for the cases shown in Fig. 3 *b*, the average shear rate in the Raman sampling region ranged from $\gamma \approx 1.4 \times 10^1\ s^{-1}$ at $\Omega = 30$ rpm to $\gamma \approx 7.0 \times 10^2\ s^{-1}$, i.e., several orders of magnitude lower than the minimum suggested by Jaspe and Hagen (9). In addition, it is clear that the different findings of individual studies, including the different results observed here in water and glycerol, indicate that there are several parameters that possibly contribute to protein unfolding. As a consequence, the question of whether protein molecules unfold in shear flow is an intriguing one and not as straightforward as it seems. It may be that the results Jaspe and Hagen observed were due to the particular protein, solvent, stress distribution, and exposure times that were used in their study. A thorough examination of the effect of these parameters on shear-induced unfolding is required to clarify the circumstances in which denaturation occurs and the structural changes that each protein experiences.

One issue highlighted by this study is that of fluid shear characterization. Aside from the difficulties associated with describing the shear in complicated flows, the choice of measure is itself problematic. Previous studies of flow-induced protein unfolding have used different parameters to describe the shear conditions, although shear rate is probably the most commonly used (4,9,17,25). However, if the magnitude of shear rate, rather than shear stress, was the instigator of the increased solvent exposure of side-chain residues, then one may expect to see similar changes occurring in water and in glycerol at the same flow rates, but this is not the case for this study. On the other hand, increased shear stresses do not appear to be associated with the changes to the α-helical and β-structure because these were only observed in water. It may be that in this case, the multiple dimensionality and time dependence of the shearing and elongation, as provided by the more complicated TVF and WVF regimes, initiated structural conformations of the lysozyme backbone. Consequently, we suggest that it is preferable if future work on shear-induced protein unfolding is conducted with the shear being quantified by the three-dimensional stress tensor, rather than γ. Such an approach has been used previously to characterize the stress distribution within cell-culture bioreactors (35) and is necessary to accurately describe most physiological biomechanics from a continuum perspective (36).

CONCLUSIONS

By combining the two techniques of PIV and Raman spectroscopy, we have identified reversible conformational changes in lysozyme, in water and in 95% glycerol, and have measured the flow field for each case. The design of the experiment enabled characterization of protein behavior in situ, which was essential because of the reversible nature of the changes: no changes would have been detected had the protein structure only been recorded post shearing. Although interactions at the interface between protein and solvent molecules may be a key reason for the differences observed in 100% water and in 95% glycerol, the problem should also be considered from a continuum mechanics perspective. For instance, the more pronounced conformational changes observed in the lysozyme molecule dissolved in glycerol, particularly near the exterior of the molecule and in the α-domain may be caused by the much higher viscous shear stresses resulting from the significantly increased dynamic viscosity of the solvent. Further combining techniques such as PIV and Raman spectroscopy may open the way for a new direction in protein engineering and structural dynamics. By correlating the spatial and temporal three-dimensional stress field with its effects on the protein, it should be possible to instigate and eventually control the unfolding processes, enabling in situ monitoring of shear-induced conformational transitions. It should also be possible to establish and minimize any structural changes occurring in processes such as pumping, filtration, and mixing, essential for any biotechnological applications involving protein solutions.

This research was supported by the UK Engineering and Physical Sciences Research Council Life Sciences Interface program (EP/F007736/1, EP/F007922/1 and EP/D000696/1).

REFERENCES

1. Dumoulin, M., J. R. Kumita, and C. M. Dobson. 2006. Normal and aberrant biological self-assembly: insights from studies on human lysozyme and its amyloiogenic variants. *Acc. Chem. Res.* 39:603–610.
2. Krebs, M. R. H., D. K. Wilkins, E. W. Chung, M. C. Pitkeathly, A. K. Chamberlain, et al. 2000. Formation and seeding of amyloid fibrils from wild-type hen lysozyme and a peptide fragment from the β-domain. *J. Mol. Biol.* 300:541–549.
3. Morozova-Roche, L. A. 2007. Equine lysozyme: the molecular basis of folding, self assembly and inante amyloid toxicity. *FEBS Lett.* 581: 2587–2592.
4. Schneider, S. W., S. Nuschele, A. Wixforth, C. Gorzelanny, A. Alexander-Katz, et al. 2007. Shear-induced unfolding triggers adhesion of von Willebrand factor fibres. *Proc. Natl. Acad. Sci. USA.* 104:7899–7903.
5. Alexander-Katz, A., M. F. Schneider, S. W. Schneider, A. Wixforth, and R. R. Netz. 2006. Shear-flow-induced unfolding of polymeric globules. *Phys. Rev. Lett.* 97:138101.
6. Castelletto, V., and I. W. Hamley. 2007. β-lactoglobulin fibers under capillary flow. *Biomacromolecules.* 8:77–83.
7. Hill, E. K., B. Krebs, D. G. Goodall, G. J. Howlett, and D. E. Dunstan. 2006. Shear flow induces amyloid fibril formation. *Biomacromolecules.* 7:10–13.

8. Chen, Z., J. Lou, C. Zhu, and K. Schulten. 2008. Flow-induced structural transition in the β-switch region of glycoprotein Ib. *Biophys. J.* 95:1303–1313.
9. Jaspe, J., and S. J. Hagen. 2006. Do protein molecules unfold in a simple shear flow? *Biophys. J.* 91:3415–3424.
10. Chen, M. C., R. C. Lord, and R. Mendelsohn. 1973. Laser-excited Raman spectroscopy of biomolecules. V. Thermal denaturation of aqueous lysozyme. *Biochim. Biophys. Acta.* 328:252–260.
11. Lednev, I. K., V. V. Ermolenkov, H. Wei, and X. Ming. 2005. Raman spectrometer tunable between 193 and 205 nm for structural characterization of proteins. *Anal. Bioanal. Chem.* 381:431–437.
12. Ashton, L., L. D. Barron, B. Czamik-Matusewicz, L. Hecht, J. Hyde, et al. 2006. Two-dimensional correlation analysis of Raman optical activity data on the α-helix-to-β–sheet transition in poly(L-lysine). *Mol. Phys.* 104:1429–1445.
13. Ashton, L., L. D. Barron, L. Hecht, J. Hyde, and E. W. Blanch. 2007. Two dimensional Raman and Raman optical activity correlation analysis of the α-helix-to-disordered transition in poly(L-glutamic acid). *Analyst (Lond.).* 132:468–479.
14. Fabian, H., and P. Anzenbacher. 1993. New developments in Raman spectroscopy of biological systems. *Vib. Spectrosc.* 4:125–148.
15. Mikhonin, A. V., N. S. Myshakina, S. V. Bykov, and S. A. Asher. 2005. UV resonance Raman determination of polyproline II, extended 2.5_1-helix and β-sheet ψ angle energy landscape in poly-L-lysine and poly-L-glutamic acid. *J. Am. Chem. Soc.* 127:7712–7720.
16. Raffel, M., C. Willert, and J. Kompenhans. 1998. Particle Image Velocimetry, a Practical Guide. Springer-Verlag, Berlin, Germany.
17. Maa, Y., and C. C. Hsu. 1996. Effect of high shear on protein. *Biotechnology and Bioengineering.* 51:458–465.
18. Ameer, G. A., E. A. Grovender, B. Obradovic, C. L. Cooney, and R. Langer. 1999. RTD analysis of a novel Taylor-Couette flow device for blood detoxification. *AIChE J.* 45:633–638.
19. Curran, S. J., and R. A. Black. 2004. Quantitative experimental study of shear stresses and mixing in progressive flow regimes within annular-flow bioreactors. *Chem. Eng. Sci.* 59:5859–5868.
20. Haut, B., H. Ben Amor, L. Coulon, A. Jacquet, and V. Halloin. 2003. Hydrodynamics and mass transfer in a Couette-Taylor bioreactor for the culture of animal cells. *Chem. Eng. Sci.* 58:777–784.
21. Laurents, D. V., and R. L. Baldwin. 1997. Characterization of the unfolding pathway of hen egg white lysozyme. *Biochemistry.* 36: 1496–1504.
22. Sasahara, K., M. Demura, and K. Nitta. 2000. Partially unfolded equilibrium state of hen lysozyme studied by circular dichroism spectroscopy. *Biochemistry.* 39:6475–6482.
23. Sasahara, K., M. Demura, and K. Nitta. 2002. Equilibrium and kinetic folding of hen-egg white lysozyme under acidic conditions. *Proteins.* 49:472–482.
24. Lord, R. C., and N.-T. Yu. 1970. Laser-excited Raman spectroscopy of biomolecules II native ribonuclease and α-chymotrypsin. *J. Mol. Biol.* 51:203–213.
25. Lee, A. T., and A. J. McHugh. 1999. The effect of simple shear flow on the helix-coil transition of poly-L-lysine. *Biopolymers.* 50:589–594.
26. Spinozzi, F., M. G. Ortore, R. Sinibaldi, P. Mariani, A. Exposito, et al. 2008. Microcalorimetric study of thermal unfolding of lysozyme in water/glycerol mixtures: An analysis by solvent exchange model. *J. Chem. Phys.* 129:035101.
27. Gekko, K., and S. N. Timasheff. 1981. Mechanism of protein stabilization by glycerol: Preferential hydration in glycerol-water mixtures. *Biochemistry.* 20:4667–4676.
28. Sinibaldi, R., M. G. Ortore, F. Spinozzi, F. Carsughi, H. Frielinghaus, et al. 2007. Preferential hydration of lysozyme in water/glycerol mixtures: a small-angle neutron scattering study. *J. Chem. Phys.* 126:235101.
29. Coles, D. 1965. Transition in circular Couette flow. *J. Fluid Mech.* 21:385–425.
30. Esser, A., and R. Grossmann. 1996. Analytic expression for Taylor-Couette stability boundary. *Phys. Fluids.* 8:1814–1819.
31. Takekiyo, T., N. Takeda, Y. Isogai, M. Kato, and Y. Taniguchi. 2006. Pressure stability of the α-helix Structure in a de novo designed protein $(\alpha\text{-l-}\alpha)_2$ studied by FTIR spectroscopy. *Biopolymers.* 85:185–188.
32. Miura, T., and G. J. Thomas. 1995. Subcellular biochemistry, Vol. 24. *In* Proteins: Structure, Function and Engineering. Plenum Press, New York.
33. Maiti, C. N., M. M. Apetri, M. G. Zargorski, P. R. Carey, and V. E. Anderson. 2004. Raman spectroscopic characterization of secondary structure in natively unfolded proteins: α-synuclein. *J. Am. Chem. Soc.* 126: 2399–2408.
34. Prevelige, P. E., D. Thomas, K. L. Aubrey, S. A. Towse, and G. J. Thomas. 1993. Subunit conformational changes accompanying bacteriophage P22 capsid maturation. *Biochemistry.* 32:537–543.
35. Dusting, J., J. Sheridan, and K. Hourigan. 2006. A fluid dynamics approach to bioreactor design for cell and tissue culture. *Biotechnol. Bioeng.* 94:1196–1208.
36. Humphrey, J. D. 2001. Stress, strain and mechanotransduction in cells. *J. Biomech. Eng.* 123:638–641.